Electronic Supplementary Material (ESI) for Dalton Transactions.
This journal is © The Royal Society of Chemistry 2017

Supplementary Information

Key Role of Higher Order Symmetry and Electrostatic Ligand Field Design in the Magnetic Relaxation of Low-coordinate Er(III) Complexes **

Saurabh Kumar Singh, Bhawana Pandey, Gunasekaran Velmurugan and Gopalan Rajaraman[a]

Supplementary Information

Table S1. Selected structural-parameters of complex **1, 2,** and **3**.

Selected structural parameters	Complex **1**	Complex **2**	Complex **3**
Er–N_1 (Å)	2.23118	2.22287	2.24883
Er–N_1 (Å)	2.25056	2.37436	2.24660
Er–N_1 (Å)	2.24634	2.30658	2.24184
Er–Cl (Å)	2.52846	2.38642	2.5712
∠N_1-Er–N_2 (°)	115.2	111.01	117.6
∠N_2-Er–N_3 (°)	118.1	113.1	114.6
∠N_1-Er–N_3 (°)	115.3	116.1	116.9
∠Cl-Er–N_1 (°)	102.7	108.2	100.6
∠Cl-Er–N_2 (°)	101.9	102.9	101.1
∠Cl-Er–N_3 (°)	100.3	102.9	101.5
∠N_1-N_2–N_3–Er (°)	23.1	30.1	20.8
τ (Å)	0.45	0.61	0.43

Table S2. SHAPE computed minimal distortion from the ideal geometry in coordination number four. vTBPY stands for axially vacant trigonal bipyramid and T-4 stands for the tetrahedral geometry.

Selected structural parameters	vTBPY-4	T-4
Complex **1**	2.103	0.381
Complex **2**	2.425	0.185
Complex **3**	2.069	0.423

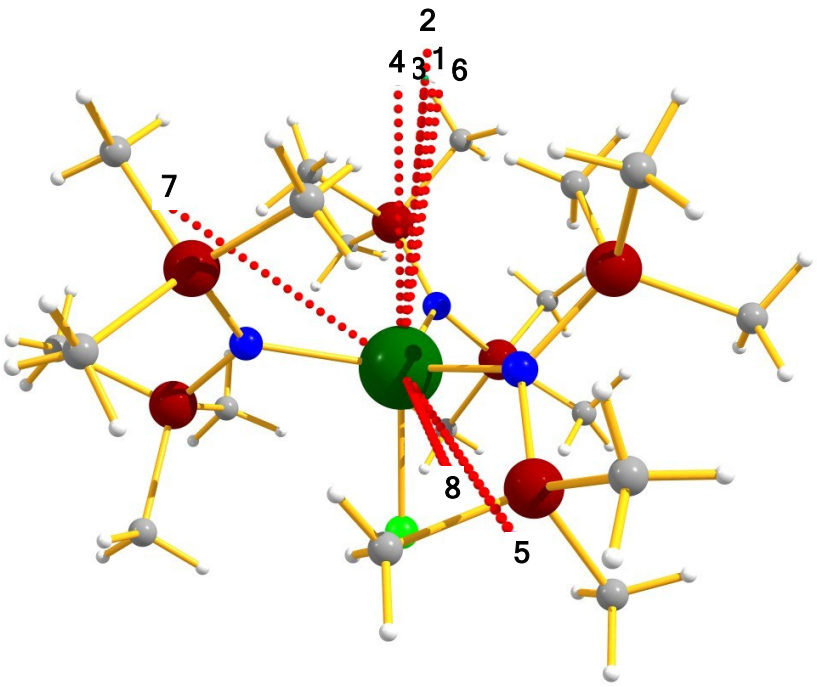

Figure S1. SINGLE_ANISO computed principal magnetization orientation of each KDs of complex **1a**.

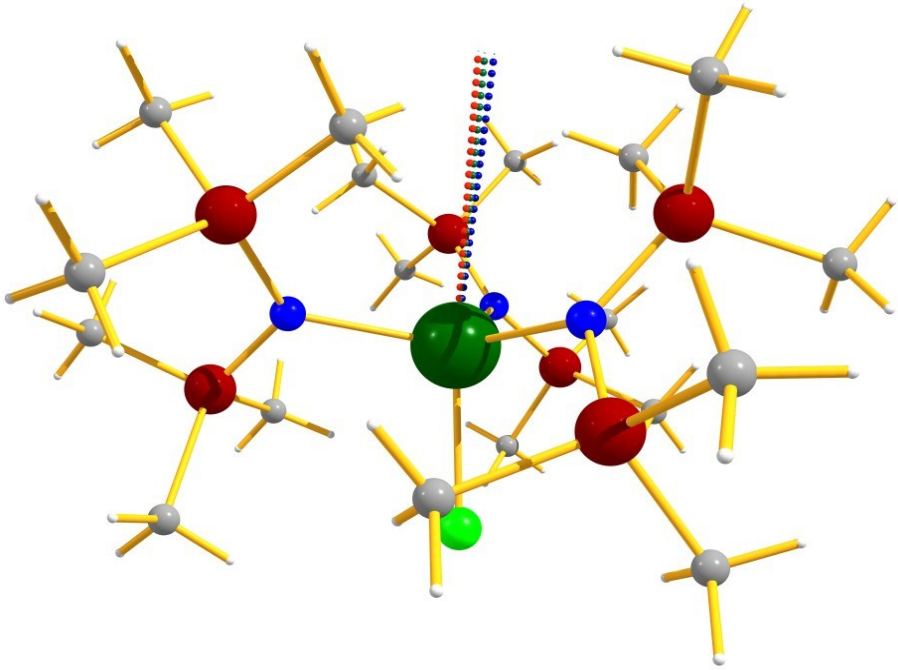

Figure S2. SINGLE_ANISO computed principal magnetization orientation of the ground state KD of complex **1a** with different level of theory. Red line represent computed orientation using BS1 basis set, Blue line represent using BS2 level of theory, green represent the computed orientation for complex 1a + 4 layers of point charge at BS1 level of theory.

Table S3. SINGLE_ANISO computed composition of wave functions of the ground *J*=15/2 of Er(III) for complex **1a**,@BS1 level of theory

	wave function 1		*wave function 2*		*wave function 3*		*wave function 4*		*wave function 5*	
m_J	*real*	*imag*	*real*	*imag*	*real*	*imag*	*real*	*imag*	*real*	*imag*
-15/2	-0.473976	0.872206	-0.000120	0.000220	-0.000254	-0.000282	-0.010734	-0.011922	0.000040	0.000017
-13/2	-0.000915	-0.006737	-0.001246	-0.000797	-0.163976	-0.080132	-0.963583	0.135742	0.014311	0.011408
-11/2	0.000050	-0.022701	-0.000302	-0.000156	-0.011238	0.000564	-0.066084	-0.050237	-0.015012	-0.017190
-9/2	-0.013635	0.105249	0.001463	0.003205	0.002609	0.013691	0.067209	0.050238	-0.007141	-0.006846
-7/2	-0.031696	0.017402	-0.001778	-0.000090	0.002511	-0.010460	-0.015089	-0.044098	-0.008230	0.018980
-5/2	0.012702	-0.005959	-0.002100	-0.000930	0.002768	0.000101	-0.009949	-0.020027	-0.013600	0.004405
-3/2	-0.010999	-0.031893	0.004476	0.006738	0.002677	0.008189	-0.005182	0.009608	-0.003122	0.003600
-1/2	0.002338	-0.005602	0.000512	0.003331	0.013199	0.005050	0.038448	-0.024400	0.063877	0.004429
1/2	0.002682	0.002041	0.006038	0.000621	-0.007592	-0.044900	0.012584	0.006430	0.017199	0.018321
3/2	-0.003783	-0.007150	-0.022771	-0.024893	0.003673	-0.010280	-0.007877	0.003490	0.032708	-0.007169
5/2	0.000186	-0.002289	0.011300	-0.008315	0.021540	-0.006006	0.001927	0.001990	-0.119346	-0.099343
7/2	-0.000770	0.001605	0.030424	-0.019540	-0.042868	0.018292	0.006093	-0.008865	0.058080	-0.082461
9/2	0.002117	0.002815	-0.098987	-0.038274	-0.082305	-0.016334	0.011921	-0.007221	0.059220	-0.152044
11/2	-0.000007	0.000340	-0.019970	-0.010796	-0.081551	-0.015499	0.007100	0.008729	-0.935046	0.229346
13/2	-0.000105	-0.001475	0.005482	0.004020	0.543853	0.806934	-0.169268	-0.068246	-0.052116	-0.040825
15/2	-0.000251	0.000000	0.992671	0.000000	-0.016042	0.000000	0.000380	0.000000	-0.018286	0.000000
	wave function 6		*wave function 7*		*wave function 8*		*wave function 9*		*wave function 10*	
-15/2	-0.016843	-0.007120	-0.005219	0.007829	0.064755	-0.097144	0.000193	-0.000530	0.003110	-0.008555
-13/2	0.063899	-0.017312	-0.012201	-0.006407	0.051728	0.061637	-0.000064	-0.028656	-0.046558	-0.044511
-11/2	-0.771968	-0.575306	0.009863	0.003293	-0.100192	-0.090502	-0.040815	0.081526	0.024475	0.033194
-9/2	0.004650	-0.163103	-0.007637	-0.111324	-0.233146	0.872117	0.061817	-0.044085	-0.121513	-0.117191
-7/2	0.021391	0.098568	0.056218	0.000833	-0.205422	0.066109	-0.263079	0.055781	-0.326979	0.706155
-5/2	0.148607	-0.045037	0.015103	0.017742	0.091945	-0.062671	0.193568	0.142530	-0.314144	0.041675
-3/2	0.027335	0.019338	-0.053278	-0.080702	-0.117269	-0.205961	-0.002165	0.134194	0.078828	-0.053920
-1/2	-0.022975	0.010179	0.001772	-0.033833	0.037255	-0.056296	0.106315	-0.116110	-0.051094	-0.245036
1/2	0.060561	0.020791	-0.067507	-0.000226	0.029134	0.017291	-0.212837	-0.131732	0.145445	-0.060251
3/2	0.001474	0.004532	0.106333	0.211815	-0.037600	-0.089094	0.077606	-0.055664	0.126860	0.043811
5/2	-0.010812	-0.009352	-0.103145	0.041745	-0.006386	-0.022407	0.146490	-0.281006	-0.067825	-0.230615
7/2	0.000191	0.020687	-0.168946	0.134260	-0.030489	0.047240	-0.775375	0.066059	0.142302	-0.228193
9/2	-0.009243	0.003525	0.854988	0.289726	0.088394	0.068101	-0.068627	-0.154238	0.062552	-0.043037
11/2	0.020520	-0.009989	0.019733	0.133565	-0.002731	0.010033	-0.022836	-0.034342	0.090565	-0.010507
13/2	0.017623	-0.004936	0.022596	0.077229	-0.001436	0.013706	-0.025927	-0.058963	0.026910	0.009850
15/2	-0.000044	0.000000	0.116748	0.000000	0.009409	0.000000	0.009102	0.000000	-0.000564	-0.000000
	wave function 11		*wave function 12*		*wave function 13*		*wave function 14*		*wave function 15*	
-15/2	-0.000177	0.000105	-0.004929	0.002939	-0.000524	0.001424	-0.003992	0.010849	-0.006431	0.000465
-13/2	0.022567	-0.003423	0.031135	0.012256	0.001560	0.002856	-0.004494	0.016413	0.017421	0.029188
-11/2	0.018778	-0.110080	-0.071589	-0.089871	0.043469	0.002147	0.027600	-0.043593	0.008897	-0.038080
-9/2	0.052401	-0.024496	-0.001924	0.080946	-0.066070	-0.158860	-0.204151	0.054442	-0.081464	-0.007831
-7/2	-0.056177	-0.208492	0.294439	-0.212568	0.072872	0.009540	0.002484	-0.000463	0.101446	0.214988
-5/2	-0.439328	-0.441623	-0.502412	0.141360	0.105900	-0.001580	-0.154308	-0.125787	-0.045363	-0.179271
-3/2	0.103641	-0.189972	-0.134003	-0.090072	-0.182390	-0.248711	-0.204662	0.759907	-0.201092	0.246123
-1/2	-0.009984	0.002476	0.224243	0.022726	0.267355	-0.145317	-0.210724	0.114181	0.707404	0.062199
1/2	0.180967	-0.134358	0.009843	-0.002986	0.179925	-0.158331	0.228701	-0.200727	-0.431119	0.093311
3/2	0.068969	-0.145989	0.186307	0.110093	-0.783835	-0.070342	-0.170427	-0.257056	0.071731	-0.106173
5/2	-0.503922	0.135878	0.151183	-0.604305	-0.064763	-0.188252	0.038052	-0.098840	-0.174963	0.166562
7/2	-0.361758	-0.031791	0.058521	0.207846	0.001292	-0.002171	-0.016212	0.071683	0.062187	-0.117850
9/2	-0.043106	-0.068540	-0.057553	0.005796	0.121591	-0.172792	0.126272	0.116864	-0.016939	0.044455
11/2	0.015465	-0.113853	0.072502	0.084933	0.050442	-0.010848	-0.012996	0.041537	0.051112	-0.048107
13/2	0.020466	-0.026472	-0.021137	0.008617	0.016955	0.001450	-0.002141	-0.002450	-0.006761	0.015154
15/2	0.005739	0.000000	-0.000206	0.000000	-0.011560	0.000000	0.001517	0.000000	-0.000000	0.000000
	wave function 16									

-15/2	-0.000000	-0.000000								
-13/2	0.007837	0.014627								
-11/2	0.054451	0.044292								
-9/2	0.020104	0.043116								
-7/2	0.070532	0.113053								
-5/2	0.186530	0.153498								
-3/2	0.079208	0.100718								
-1/2	0.436730	0.061947								
1/2	0.701069	-0.113101								
3/2	0.218334	0.230965								
5/2	-0.032304	0.182078								
7/2	-0.085662	0.221750								
9/2	-0.080686	0.013691								
11/2	-0.011623	-0.037339								
13/2	0.015269	-0.030369								
15/2	0.006448	0.000000								

Table S4. SINGLE_ANISO computed composition of wave functions of the ground *J*=15/2 of Er(III) for complex **1a** + 4 layers of point charges, @BS1 level of theory

	wave function 1		*wave function 2*		*wave function 3*		*wave function 4*		*wave function 5*	
m_J	*real*	*imag*	*real*	*imag*	*real*	*imag*	*real*	*imag*	*real*	*imag*
-15/2	0.000067	-0.000007	0.989014	-0.103423	0.012647	-0.000303	-0.000002	0.000000	-0.013448	-0.019088
-13/2	-0.000829	0.000608	0.004198	-0.002810	-0.659336	0.725667	-0.115212	0.092456	-0.064497	-0.044892
-11/2	0.000028	-0.000098	-0.025805	0.000823	0.092556	0.004632	0.003547	-0.004990	0.003147	-0.966836
-9/2	0.002676	0.000088	-0.089622	0.027394	0.067297	0.005605	0.008977	0.003850	-0.119850	0.106372
-7/2	0.000580	-0.000752	0.022665	0.015361	0.024623	0.026033	0.004426	0.005814	-0.060320	0.051216
-5/2	-0.001658	0.000490	0.002692	0.007543	-0.011582	-0.007654	0.001564	-0.000385	-0.086914	-0.113392
-3/2	-0.006112	-0.001443	-0.025745	0.011367	0.004229	-0.009723	-0.005255	-0.002197	-0.003066	0.026659
-1/2	0.002228	0.000980	0.004054	0.000416	0.029788	-0.026757	0.011467	-0.002813	0.009552	0.019165
1/2	-0.003989	0.000836	0.002114	-0.001206	-0.011531	-0.002538	0.030421	0.026035	-0.013646	0.058303
3/2	-0.026788	-0.008628	0.005929	-0.002071	-0.005201	0.002323	-0.004461	-0.009619	0.004272	-0.006139
5/2	-0.001893	0.007782	-0.001700	-0.000315	-0.001573	-0.000347	-0.011395	0.007929	0.004724	-0.012828
7/2	0.020945	-0.017634	-0.000655	-0.000688	0.004285	-0.005919	-0.023991	0.026616	0.012360	0.004107
9/2	0.091985	0.017925	0.002652	-0.000366	-0.008883	0.004064	0.067143	-0.007218	0.004017	-0.006302
11/2	-0.025750	0.001866	-0.000038	-0.000094	0.003666	0.004904	-0.092418	0.006851	0.027187	-0.002739
13/2	-0.004468	-0.002358	-0.000887	-0.000519	0.117396	0.089666	-0.676549	-0.709646	-0.004027	0.012264
15/2	0.994407	0.000000	-0.000068	0.000000	-0.000002	0.000000	-0.012650	0.000000	0.000499	0.000000
	wave function 6		*wave function 7*		*wave function 8*		*wave function 9*		*wave function 10*	
-15/2	-0.000288	-0.000408	-0.003405	-0.001385	-0.093714	-0.038125	0.000979	0.004317	-0.000823	-0.003629
-13/2	0.007707	-0.010356	0.002534	-0.003559	-0.047126	0.050016	-0.030048	0.011490	0.043188	0.022541
-11/2	-0.013419	-0.023803	0.000570	0.000457	-0.104650	0.081495	-0.011732	0.024185	0.028175	0.079418
-9/2	-0.002839	0.006913	0.014185	-0.012945	-0.893198	-0.230506	-0.133163	0.006212	0.034887	0.103331
-7/2	-0.010476	-0.007739	0.030934	-0.010807	0.088443	0.186200	-0.223411	-0.490042	-0.213839	0.618237
-5/2	-0.007766	0.011250	-0.024517	0.006170	0.035898	0.079410	-0.294362	0.196245	-0.032550	-0.127088
-3/2	0.002558	-0.007028	-0.112606	-0.022713	-0.208790	0.058650	0.019847	0.090371	0.072915	0.061202
-1/2	0.039803	-0.044734	0.026301	0.028913	0.039204	0.031888	-0.136502	-0.086625	-0.013008	0.234032
1/2	-0.021168	0.003229	-0.048330	0.014764	0.035257	-0.016870	-0.225355	0.064460	-0.114677	-0.113955
3/2	0.020028	-0.017860	-0.171297	-0.133005	0.112864	0.021394	0.075816	0.057569	-0.092523	0.000638
5/2	0.142754	0.005745	-0.063176	0.060029	-0.020385	-0.014954	0.131140	0.003628	0.126260	-0.330484
7/2	0.007128	-0.078809	0.152089	-0.139146	-0.024582	-0.021667	0.555610	-0.345314	0.527325	0.109462
9/2	-0.017933	0.159240	0.914215	0.123070	0.008262	0.017336	-0.108489	-0.011162	-0.023402	-0.131238
11/2	-0.788569	0.559411	-0.066226	-0.114922	-0.000700	0.000208	0.083683	0.009907	-0.020990	0.016792
13/2	0.073845	0.026871	0.024804	0.064088	0.001007	0.004251	-0.031537	-0.037131	0.004558	-0.031845
15/2	-0.023350	-0.000000	-0.101172	0.000000	0.003676	0.000000	-0.003721	0.000000	-0.004427	0.000000
	wave function 11		*wave function 12*		*wave function 13*		*wave function 14*		*wave function 15*	
-15/2	-0.001966	0.003471	-0.000326	0.000575	0.009621	0.005438	0.000610	0.000345	-0.000000	0.000000
-13/2	-0.029122	0.002421	-0.009989	0.012911	-0.011236	-0.010687	-0.001778	0.001917	-0.014918	0.006417
-11/2	-0.089315	-0.039298	-0.078813	-0.074727	-0.016678	-0.050041	0.020803	-0.025445	0.052232	-0.023562
-9/2	0.004162	-0.077287	-0.001374	0.032431	0.064538	-0.198977	0.147925	0.007826	-0.042167	-0.008487
-7/2	0.237745	-0.271660	-0.138989	-0.088204	0.025813	0.025113	0.035024	-0.037582	0.150824	-0.002446
-5/2	0.426724	-0.266712	0.670603	0.009427	0.167456	0.033755	-0.082878	0.064535	-0.211679	0.028403
-3/2	-0.161072	-0.028891	-0.068305	-0.165987	0.402203	0.707726	-0.298558	-0.062972	0.142108	0.024376
-1/2	-0.224587	-0.006011	0.024097	0.002056	0.043554	-0.217210	-0.091600	0.269635	-0.400837	0.318286
1/2	0.010088	-0.021980	0.105461	-0.198377	0.052944	-0.279804	0.068973	-0.210523	0.538578	-0.419236
3/2	-0.110761	-0.141242	-0.054249	0.154389	0.290896	0.092099	0.698402	-0.418184	-0.290388	-0.023218
5/2	0.322315	-0.588141	-0.442385	0.239842	-0.040392	-0.096964	-0.162388	-0.053019	0.078884	0.182910
7/2	-0.008244	-0.164408	0.353549	-0.072971	-0.011996	-0.049952	0.034829	-0.009159	0.013123	-0.213623
9/2	-0.028895	-0.014788	-0.069299	-0.034471	0.132626	0.065980	0.041732	-0.204977	-0.055179	0.047012
11/2	-0.026176	-0.105406	-0.009827	0.097082	-0.005588	-0.032388	-0.039144	0.035355	0.011767	0.034083
13/2	-0.016157	0.002328	0.016460	-0.024146	-0.000605	-0.002544	0.015041	-0.003774	0.013617	-0.022945
15/2	0.000661	0.000000	-0.003990	0.000000	-0.000701	0.000000	0.011052	0.000000	-0.005222	0.000000
	wave function 16									

-15/2	-0.003761	0.003623								
-13/2	-0.025726	-0.007076								
-11/2	-0.015174	-0.032709								
-9/2	0.072355	-0.004429								
-7/2	0.157668	0.144733								
-5/2	0.070100	0.186453								
-3/2	-0.193012	0.218198								
-1/2	-0.678730	0.071770								
1/2	-0.509495	0.048899								
3/2	-0.085425	0.116153								
5/2	-0.172145	0.126414								
7/2	-0.110313	0.102884								
9/2	-0.024478	0.035368								
11/2	-0.053962	0.019272								
13/2	-0.015195	0.005730								
15/2	0.000000	0.000000								

Table S5. CASSCF+RASSI computed low-lying energies of eight KDs and associated g-tensors along with the deviation from the principal magnetization axes for complex **1a** with experimental geometry + 4 layers of point charges@BS1 level of theory.

J multiplet	Energies of KDs	g_{XX}	g_{yy}	g_{zz}	θ
$^4I_{15/2}$	0.00	0.012094	0.015622	17.83155	-
	43.489	0.169797	0.185678	15.47051	3.8
	87.625	0.130957	0.208802	12.8733	5.1
	140.706	0.74469	0.829385	10.17223	5.8
	194.393	6.663329	6.146718	5.134495	107.6
	286.802	5.990632	5.825627	3.781628	7.4
	337.393	5.300763	4.092423	2.53549	29.2
	374.963	0.862937	4.759339	13.62414	87.3

Table S6. SINGLE_ANISO computed crystal field parameters of complex **1a** and **1** along with experimental geometry + 4 layers of point charges on complex **1a**@ BS1 level of theory.

		Complex **1a**@BS1level	Complex **1**@BS1level	Complex **1a** + 4 layers of point charges@ BS1level
k	q	B_q^k		B_q^k
2	-2	0.1393E+00	0.2548E+00	0.1662E+00
	-1	-0.6100E+	-0.4451E+00	0.5757E+00
	0	00	**-0.2025E+01**	**-0.2086E+01**
	1	**-0.1861E+01**	-0.7480E+00	0.3969E+00
	2	-0.3198E+00	0.8028E-01	0.2434E+00
		0.2322E+00		
4	-4	0.2129E-02	0.1015E-02	0.2001E-02
	-3	**-0.3783E-01**	-0.5741E-02	**0.2874E-01**
	-2	0.2220E-02	0.2361E-02	0.2169E-02
	-1	0.4983E-02	0.2920E-02	-0.4196E-02
	0	0.2427E-02	0.2708E-02	0.2546E-02
	1	0.1747E-02	0.4812E-02	-0.2391E-02
	2	0.8557E-03	-0.1771E-02	0.5322E-04
	3	**0.2971E-01**	**0.4772E-01**	**-0.3736E-01**
	4	0.1889E-02	0.3092E-03	0.6654E-03
6	-6	**-0.1241E-03**	**0.2125E-03**	-0.2258E-05
	-5	0.9443E-04	-0.1424E-04	-0.8952E-04
	-4	-0.3122E-04	-0.4003E-04	-0.3158E-04
	-3	**0.2291E-03**	-0.3595E-04	**-0.1647E-03**
	-2	-0.4617E-04	-0.2798E-04	-0.4172E-04
	-1	-0.1482E-04	0.2628E-05	0.4486E-05
	0	-0.5076E-05	-0.4135E-05	-0.4636E-05
	1	0.5294E-05	-0.3985E-05	-0.1692E-05
	2	-0.1717E-04	0.4374E-04	-0.5501E-06
	3	**-0.2707E-03**	**-0.3550E-03**	**0.3231E-03**
	4	-0.4299E-04	-0.2761E-04	-0.2960E-04
	5	0.9535E-04	-0.5276E-04	-0.7555E-05
	6	**0.1929E-03**	0.5941E-04	**0.2276E-03**

*It is important to note here that charges on complex **1a** are computed in presence of all the solvent and counter ions.*

Table S7. CASSCF+RASSI computed low-lying energies of eight KDs and associated g-tensors along with the deviation from the principal magnetization axes for complex **1a** @BS2 level of theory.

J multiplet	Energies of KDs	g_{XX}	g_{yy}	g_{zz}	θ
$^4I_{15/2}$	0.000	0.02485	0.03062	17.79175	-
	30.7	0.18646	0.19876	15.41854	5.4
	65.4	0.07937	0.31195	12.80838	6.5
	113.0	0.74406	0.94597	10.19707	8.538
	162.8	6.86911	6.09884	5.11913	114.494
	254.7	3.69893	5.12169	6.91675	87.518
	304.5	2.14421	3.57783	5.19745	65.414
	339.7	0.92027	5.37676	13.12406	86.142

Table S8. CASSCF computed low-lying energies of eight KDs and associated g-tensors along with the deviation from the principal magnetization axes for complex **2** @BS1 level of theory.

J multiplet	Energies of KDs	g_{XX}	g_{yy}	g_{zz}	θ
$^4I_{15/2}$	0.0	0.02389	0.06855	17.63897	-
	27.9	0.09206	0.20378	16.86069	33.2
	43.6	0.25222	0.57703	13.17897	26.6
	76.2	2.32995	2.76825	9.51393	19.7
	113.4	4.24816	4.99053	8.68748	87.3
	170.9	0.21188	1.87251	14.734150	63.8
	226.6	0.72766	1.20289	13.56825	87.2
	268.6	0.139209	0.42886	16.44025	82.1

Table S9. CASSCF+RASSI computed low-lying energies of eight KDs and associated g-tensors along with the deviation from the principal magnetization axes for complex **1m**@BS1 level of theory

J multiplet	Energies of KDs	g_{XX}	g_{yy}	g_{zz}	θ
$^4I_{15/2}$	0	0.00142	0.001668	17.87679	-
	161.426	0.05581	0.058184	15.47771	0.966
	261.512	0.014765	0.086832	13.00148	0.13
	350.14	0.310112	0.381418	10.42494	2.026
	439.757	4.188673	4.791167	7.086456	3.622
	557.428	5.055701	4.709003	3.871031	91.904
	639.055	2.793524	2.861461	4.80817	57.89
	693.349	0.971017	5.731619	12.90281	89.765

Table S10. CASSCF computed low-lying energies of eight KDs and associated g-tensors along with the deviation from the principal magnetization axes for complex $\mathbf{1_{TP}}$.

J multiplet	Energies of KDs	g_{XX}	g_{yy}	g_{zz}	θ
$^4\mathbf{I}_{15/2}$	0	0.0019	0.00217	17.8707	-
	51.423	0.199036	0.200086	15.51083	1.45
	85.907	0.157348	0.215567	13.04715	1.161
	135.075	0.066175	0.126305	10.5707	0.838
	198.806	4.054621	4.218459	7.381226	1.515
	285.643	4.108186	4.223895	5.007952	3.613
	349.839	0.83886	0.955221	3.519031	3.364
	388.713	10.4111	8.612665	1.130831	0.391

Table S11. CASSCF computed low-lying energies of eight KDs and associated g-tensors along with the deviation from the principal magnetization axes for complex $\mathbf{1_{TD}}$.

J multiplet	Energies of KDs	g_{XX}	g_{yy}	g_{zz}	θ
$^4\mathbf{I}_{15/2}$	0	0.521027	0.600991	15.09973	-
	15.492	0.383663	0.658684	12.12932	4.609
	35.829	0.471203	0.670606	11.61557	9.081
	55.915	1.227529	1.569372	14.53961	5.403
	62.078	3.248159	5.894158	9.85356	93.561
	147.307	9.375779	6.484333	1.479679	6.816
	161.036	4.936655	3.07825	0.239851	83.779
	172.334	11.27383	6.934004	0.950846	3.106

Table S12. CASSCF computed low-lying energies of eight KDs and associated g-tensors along with the deviation from the principal magnetization axes for complex $[Dy\{N(SiMe_3)_2\}_3Cl]^-$

J multiplet	Energies of KDs	g_{XX}	g_{yy}	g_{zz}	θ
$^6\mathbf{H}_{15/2}$	0	0.664631	2.47276	17.56988	-
	54.226	3.262879	6.110436	9.045304	65.445
	123.096	0.559939	3.065325	6.603197	90.521
	233.874	1.617658	1.837447	9.421955	90.168
	377.023	0.142617	0.17994	12.2051	89.956
	544.323	0.004236	0.031898	14.65061	90.165
	689.929	0.015824	0.018622	17.24196	90.32
	773.974	0.00136	0.001667	19.78676	87.518

Table S13. CASSCF computed low-lying energies of eight KDs and associated g-tensors along with the deviation from the principal magnetization axes for complex $[Er\{N(SiMe_3)_2\}_3F]^-$

J multiplet	Energies of KDs	g_{XX}	g_{yy}	g_{zz}	θ
$^4I_{15/2}$	0	0.121108	0.579042	15.9838	-
	16.383	0.080433	0.402355	14.43767	45.328
	45.289	0.799808	1.201271	10.08905	31.795
	89.167	5.232643	5.7497	7.720941	72.383
	112.052	0.067618	0.083286	17.62166	34.535
	174.819	7.664634	5.709663	3.023434	27.814
	210.499	6.555538	4.594337	2.165944	28.554
	240.277	0.716746	3.798668	14.2454	78.523

Table S14. CASSCF computed low-lying energies of eight KDs and associated g-tensors along with the deviation from the principal magnetization axes for complex $[Er\{N(SiMe_3)_2\}_3Br]^-$

J multiplet	Energies of KDs	g_{XX}	g_{yy}	g_{zz}	θ
$^4I_{15/2}$	0	0.01022	0.011443	17.83325	-
	57.711	0.18898	0.204022	15.44414	0.583
	99.813	0.103583	0.274152	12.81948	2.09
	146.593	0.750785	0.880973	10.11515	4.295
	195.211	5.252219	6.037408	6.922933	95.919
	289.116	6.180879	6.064181	3.656912	4.826
	339.438	5.129795	3.94612	2.493783	32.505
	376.757	0.886134	4.974724	13.43618	88.43

Table S15. CASSCF computed low-lying energies of eight KDs and associated g-tensors along with the deviation from the principal magnetization axes for complex $[Er\{N(SiMe_3)_2\}_3I]^-$

J multiplet	Energies of KDs	g_{XX}	g_{yy}	g_{zz}	θ
$^4I_{15/2}$	0	0.005996	0.006311	17.85143	-
	75.558	0.15372	0.162951	15.46165	1.196
	126.829	0.078098	0.222511	12.85004	1.465
	178.584	0.712607	0.822698	10.12619	2.209
	230.973	6.728171	6.123033	5.20345	109.178
	326.11	6.136628	5.836204	3.753061	6.124
	378.756	5.032003	3.989519	2.502101	34.406
	417.494	0.891076	5.005495	13.41989	88.808

Table S16. CASSCF+NEVPT2 computed low-lying spin-free states and spin-orbit states along with the ground state g-tensor for complex $[Er\{N(SiMe_3)_2\}_3F]^-$.

CASSCF computed spin-free states			NEVPT2 computed spin-free states			NEVPT2 computed energies of low-lying eight KDs.
0.8	24327.5	43457	2	23717.3	42044.2	0
32.7	24410.1	43473.7	16.4	23874.5	42067.5	0
37.8	24415.5	43495.1	23.1	23893.8	42079.2	15.6491
72.9	24460.1	43501.5	36.9	24066.8	42098.4	15.6491
136	24503.8	47528.9	99.4	24168	45632.5	42.6452
139.5	24511.4	47531.2	104.2	24198.4	45633.7	42.6452
156.6	29350.4	47568.3	139.5	28002	45730.8	83.1577
186.8	29353.1	47582.5	226.7	28010.7	45738.3	83.1577
193.2	29371.8	47595.7	238	28117.7	45751.1	108.7098
229.5	29445.2	47615.8	332.1	28135.9	45796.3	108.7098
242	29452.3	47627.3	347.7	28176.6	45808.7	219.4431
255.5	29467.4	47634.8	381	28183.3	45810.1	219.4431
13075.2	29506.5	47649.8	12671.3	28348.2	45849.3	291.8797
13095.2	29513.3	47665.5	12693.8	28370.8	45868.7	291.8797
13099.9	35467.2	47677.4	12699.9	33415.8	45883.9	345.6315
13128	35475.5	50852.7	12765.5	33432.6	47930	345.6315
13132.7	35476.9	50873.6	12770	33435.8	47946.2	Main value of g-tensor (NEVPT2)
13196.1	35644.2	50880	12817.5	33662.2	47947	
13199.7	35651.5	50890.5	12818.3	33676.8	47981.1	g_{zz} = 16.468435
13230.6	35717.7	50934.5	12839.7	33728.2	48063.1	g_{yy} = 0.597440
13239.9	35731.6	50944.9	12847.8	33755.3	48077.3	g_{xx} = 0.156503
13257.4	35744.6	50957.4	12884	33815	48081	
13257.9	35793.9	51349.4	12884	33904.7	48928.4	
22114.2	41625	51384.3	21313.9	39619.8	48941	
22138.8	41625	51435	21349.5	39619.8	49092.3	
22155.3	41799.8	51503.3	21365.9	39964.2	49103.9	
22226.8	41799.8	51539.5	21459.9	39964.2	49143.8	
22234.1	41925.6	57943.2	21471	40231.8	54651.3	
22287.5	41925.8	57985.2	21479.6	40232	54690.9	
22291.6	42040.8	58262.8	21490.8	40492.7	55510.5	
22321.8	42041.9	58422.9	21544.3	40493.1	55646.9	
22327.9	42144.5	58507	21564.4	40735.3	55657.5	
22596.3	42151	82098.2	21596.1	40739.2	78400.5	
22608.7	42225.7	82100.4	21637.3	40966.4	78400.8	
22662.5	42245.1	82169.9	21637.4	40993.7	78605.5	
22680	42282.8	82214.9	21646.8	41002.9	78660.5	
22714.5	42321.8	82298.1	21655.3	41006.2	78852.9	
22715.7	42331.8	82304.3	21784.2	41008.2	78862.7	
22845.8	42398.9	82347.5	21863.6	41157.7	78953.6	
22922.1	42399.7	82359.5	21923.5	41162.8	79009.3	

24019.1	43162.7	82372.8	23109.3	41522.4	79010.4	
24019.5	43162.7	111260.3	23109.5	41522.5	105840	
24098	43325.9	111390.1	23210.7	41854.5	105983.1	
24098.7	43335.7	111781.1	23211.1	41870.2	106882.8	
24129.7	43341.2	111867.3	23231.7	41909.4	106915.9	
24130.1	43346.8	111913.3	23232.6	41926.3	107085.5	
24210.3	43371.2	112034.4	23482.9	41928.6	107217.8	
24212	43413.7	112066.9	23485.5	41974.5	107285.5	
24310.2	43416.1		23693.5	41988.4		

Table S17. CASSCF+NEVPT2 computed low-lying spin-free states and spin-orbit states along with the ground state g-tensor for complex $[Er\{N(SiMe_3)_2\}_3Cl]^-$.

CASSCF computed spin-free states			NEVPT2 computed spin-free states			NEVPT2 computed energies of low-lying eight KDs.
1	24487.5	43614.9	3.6	23812.5	42286.9	0
44.6	24606.2	43632	59.4	23936.7	42298.5	0
45.1	24611	43664.2	60.4	23943.4	42335.1	55.4486
89.2	24671.9	43666.8	62.4	24007.5	42339.2	55.4486
93.5	24720.5	47528	66.1	24056.8	45861.6	74.736
136.1	24731.1	47528.6	77.3	24067.5	45862.7	74.736
205.5	29313.6	47615	163.7	28174.3	45934.2	104.2855
257.8	29325.6	47618.6	245.5	28181.5	45937.3	104.2855
261.4	29329.7	47660.9	254.5	28255.6	45993.5	162.6404
318.5	29439.7	47700.8	359.6	28260.1	46031.3	162.6404
336.8	29500.3	47729.7	381.3	28319.1	46061.1	265.9998
355.9	29508.4	47732.7	420	28329.3	46064.1	265.9998
13084.5	29647.8	47754.6	12714.7	28543.6	46083.3	342.8371
13103.2	29653.9	47771.4	12728.8	28560.4	46098.6	342.8371
13108.9	35560.3	47777.4	12733.2	33686.2	46102.7	399.1787
13161.7	35561.8	50733.6	12778.3	33690.3	48165.9	Main value of g-tensor (NEVPT2)
13168.8	35574	50735.1	12784.6	33749	48224.7	
13244.8	35703	50847.6	12855.1	33872.8	48253.1	g_{zz} = 17.884149
13252.7	35705.9	50877.8	12863.7	33875.3	48258.7	g_{yy} = 0.004298
13277.2	35737.8	50967.6	12884.4	33938.3	48338.5	g_{xx} = 0.002807
13277.6	35744.7	50987.3	12885.1	33946.1	48351	
13298.6	35769.9	51056.6	12906.4	33972.7	48410	
13299.2	35821.5	51485.6	12907	34062.2	49120.7	
22064.8	40995.7	51505.8	21380.3	39678.6	49136.3	
22101	40995.7	51627.6	21413.6	39678.6	49389.9	
22120.4	41424	51661.9	21432.4	40069.2	49411.2	
22226.5	41424.1	51701	21532.1	40069.2	49424.3	
22232.7	41768.3	57709.6	21537	40400.3	54929.6	
22376	41768.5	57734.6	21619.8	40400.6	54963.6	
22380.1	42053.1	58588.6	21638.3	40676.1	55837.2	
22490.6	42053.6	58659.9	21663.8	40677.1	55901.7	
22490.8	42284	58717.5	21670	40903.1	55909	
22609	42288.6	81941.8	21673.1	40911.7	78794.2	
22613.4	42457.2	81943.2	21678.2	41072.8	78795.8	
22638.4	42477.3	82163	21683.4	41106.8	79020.8	
22666.7	42578	82211.6	21793.1	41205.6	79072.5	
22683.4	42610.3	82404.9	21793.3	41237.4	79249.3	
22755	42648.4	82406.4	21952.2	41277.3	79250.4	
22979.8	42727.9	82527.9	22008.1	41359.9	79375.2	
23029.6	42732.4	82560.9	22070.8	41363.7	79408.5	

23741.8	43074	82590.1	23097.5	41738.3	79439.6	
23741.9	43074.2	110787.8	23097.5	41738.3	106392.2	
23904	43287.8	110920.4	23226.8	41959.9	106531.6	
23904.5	43287.9	111859.9	23227.4	41960.1	107452.5	
24100.8	43444.4	111888.6	23411	42133	107487.1	
24100.9	43445.9	112340	23411.2	42136.2	107918.9	
24300.6	43536.8	112444.4	23615.9	42210.2	108025.2	
24302.7	43552	112543.1	23618	42239.1	108072.2	
24467.1	43596.8		23790.9	42262.3		

Table S18. CASSCF+NEVPT2 computed low-lying spin-free states and spin-orbit states along with the ground state g-tensor for complex $[Er\{N(SiMe_3)_2\}_3Br]^-$.

CASSCF computed spin-free states			NEVPT2 computed spin-free states			NEVPT2 computed energies of low-lying eight KDs.
1	24534.6	43675.8	3.1	23377.6	40989.9	0
67.3	24659.5	43702.9	106.2	23526.3	41015.3	0
67.6	24664.3	43734.4	106.3	23534	41059.1	93.4711
115.4	24728	43738.8	107.7	23613.4	41061.7	93.4711
119.8	24776.8	47550.6	112.7	23672.2	44144.3	122.9477
162.6	24788.1	47551.1	121.4	23678.9	44145	122.9477
235	29324.5	47643	192.6	27041.5	44235.8	150.4914
289.2	29339.9	47646.6	301.2	27051.9	44238.8	150.4914
292.7	29344.4	47699.1	313.6	27111.7	44324.4	213.9123
353.1	29459.4	47739.1	441.6	27140.2	44359.2	213.9123
371.9	29526.8	47770.8	467.2	27190.8	44397.9	327.8859
392.3	29534.6	47773.6	512.4	27201.9	44400.4	327.8859
13105.2	29692.4	47794.8	12551	27476.2	44419.4	421.9603
13123.6	29698.4	47811.5	12564.1	27498.3	44437.4	421.9603
13129.2	35592.4	47816.4	12568.1	32193.1	44438.9	Main value of g-tensor (NEVPT2)
13182.7	35593.7	50728.5	12614.6	32197.5	46258.2	
13189.9	35608.7	50729.5	12621.1	32265.7	46311.9	g_{zz} = 17.883549
13266.3	35727.4	50866.7	12692.8	32385.9	46319.2	g_{yy} = 0.002194
13273.7	35732.8	50899	12702.9	32393	46324.6	g_{xx} = 0.001815
13313.5	35770.7	50989.7	12745	32465.5	46432.9	
13313.9	35776.1	51010.1	12745.6	32469.4	46448.1	
13325.1	35798.3	51097.9	12754.1	32517.8	46542.4	
13325.8	35851.8	51535.1	12754.8	32608.4	47247.4	
22076.1	40913.2	51554.1	20688.1	38172.5	47260.1	
22114.2	40913.2	51682.2	20728.8	38172.5	47517.3	
22133.8	41382.4	51716	20761.1	38594.2	47546.4	
22245.7	41382.4	51755.1	20771.5	38594.2	47555.3	
22251.8	41763.3	57692.1	20789.9	38977.8	52374	
22407	41763.5	57716	20944.8	38978.2	52408.8	
22410.5	42074.1	58641	20983.7	39298.7	53452.7	
22541.8	42074.6	58712.1	20994.3	39299.5	53530.4	
22542	42323	58809.8	21003.5	39566.3	53580.8	
22619.2	42327.8	81939	21115.8	39573.3	75516.3	
22623.9	42507.9	81940.4	21120.1	39768.8	75517.6	
22651.8	42529.3	82184.8	21176.6	39800.4	75803.8	
22692.7	42637.2	82234.7	21229.8	39936.6	75855.9	
22707.1	42668.4	82444.6	21283	39954.3	76074.4	
22781.1	42710	82446.1	21287.7	40009.2	76074.6	
23019.5	42789.7	82581.8	21447.6	40122.1	76236	
23070.3	42794.8	82615.6	21447.9	40128.5	76274.2	

23704.1	43080	82650.9	22506.3	40269.2	76313	
23704.1	43080.1	110734.3	22506.4	40269.2	101847.8	
23898	43297.7	110868.4	22673	40515.7	101984.7	
23898.5	43297.8	111892.9	22673.5	40515.9	103059.7	
24119.6	43473.1	111918.7	22899.5	40753.5	103091.1	
24119.8	43474.1	112436.4	22899.8	40755.4	103711.9	
24336.6	43586.1	112538.2	23145.9	40889.5	103825.5	
24338.6	43598.5	112650.5	23148.1	40906.1	103871	
24513.9	43662		23354.7	40972.1		

Table S19. CASSCF+NEVPT2 computed low-lying spin-free states and spin-orbit states along with the ground state g-tensor for complex $[Er\{N(SiMe_3)_2\}_3I]^-$.

CASSCF computed spin-free states			NEVPT2 computed spin-free states			NEVPT2 computed energies of low-lying eight KDs.
0.9	24591.2	43753.2	2.6	23794.3	41934.6	0
90.4	24725.6	43794.8	139.9	23951.5	41970.6	0
90.6	24730.5	43826	140.3	23958.9	42013	122.3681
147.1	24798.9	43834	141.3	24042.1	42016.4	122.3681
151.4	24848.6	47574.2	146.1	24101.4	45235.5	158.3934
198.3	24860.9	47574.6	154	24109.1	45236.1	158.3934
271.1	29333.2	47676.1	230.4	27705.7	45330.6	187.8547
328.5	29352.2	47679.6	342.5	27710.5	45333.3	187.8547
332	29357.1	47743.2	355.5	27737.8	45435.2	254.1653
395.5	29480.9	47782.8	489.9	27795.6	45472	254.1653
414.7	29555.8	47817.6	516.6	27908.6	45516	373.1904
436.2	29563.3	47820.3	564.3	27919.4	45518.1	373.1904
13127.2	29745.6	47840.9	12715.7	28146.7	45536.4	472.1602
13145.7	29751.6	47857.6	12727.9	28162.9	45553.8	472.1602
13151.3	35628	47861.6	12731.8	33095.5	45554.7	543.3232
13206.2	35628.9	50712.8	12778	33099.6	47367.1	543.3232
13213.4	35644.1	50713.5	12784.2	33172.3	47397.8	Main value of g-tensor (NEVPT2)
13291.5	35757	50885.5	12856.6	33277.3	47422.8	
13298.3	35763.8	50918.1	12866	33287.4	47549.4	g_{zz} = 17.885379
13353.1	35807.2	51012.2	12918.7	33365	47566.4	g_{yy} = 0.001238
13353.1	35811.9	51033.4	12919	33367.5	47678.2	g_{xx} = 0.001132
13361.3	35833	51143.7	12928.3	33419.2	48384.2	
13361.8	35887.3	51594.5	12928.5	33510.5	48396.7	
22085.2	40796.9	51612.5	21221.3	38942.2	48666.5	
22126.2	40796.9	51746.3	21235.9	38942.2	48706.5	
22146.1	41321.4	51782.3	21271.4	39429.2	48712	
22266.6	41321.4	51821.9	21277.3	39429.2	53753.1	
22272.5	41748.6	57659.9	21297.6	39863.5	53789.2	
22443.9	41748.8	57682.8	21303	39863.9	54933.3	
22446.8	42092.8	58704.6	21322.5	40213.3	55010.9	
22604.3	42093.2	58775.3	21340.3	40214.2	55098.1	
22604.4	42365	58921.8	21417.2	40498.1	77398.6	
22624.4	42369.6	81925.4	21421.1	40505.3	77399.9	
22636.4	42565.2	81926.7	21534.4	40709.7	77713.9	
22663.3	42587	82202.6	21598.5	40743.6	77768.5	
22719.7	42704.3	82253.5	21603.6	40881.8	78012.1	
22732.5	42734.8	82487.7	21753.5	40902.2	78012.8	
22810.6	42780.8	82489.2	21791.6	40959	78197.1	
23068.5	42861	82643	21791.9	41067.2	78236.3	
23118.8	42866.8	82677.9	21810.6	41073.4	78285	

23651.3	43080.2	82720.1	22808.7	41118.7	104294.6	
23651.3	43080.3	110650.6	22808.7	41118.7	104435.9	
23884.1	43306.4	110785.5	23018.4	41382	105631.7	
23884.6	43306.6	111925.8	23018.9	41382.3	105663.1	
24137.4	43505.7	111949.3	23278.1	41654.4	106353.1	
24137.5	43506.5	112548	23278.3	41655.9	106464.7	
24377.3	43644.8	112648.7	23547.5	41820.9	106523.7	
24379.3	43655.6	112780.6	23549.7	41832.2		
24569.9	43743.1		23771.2	41921.1		

Table S20. Reduced LOEWDIN POPULATION ANALYSIS on model complexes $[Er\{N(SiMe_3)_2\}_3X]^-$ (where X = F, Cl, Br and I). The Er is considered in +III oxidation state, while halide is considered as X^- ion. The numbers provided here are net gain/loss of electron compared to reference (electronic structure of ions). The negative and positive sign here are the loss and gain of the electrons from reference electronic structure.

	$[Er\{N(SiMe_3)_2\}_3F]^-$	$[Er\{N(SiMe_3)_2\}_3Cl]^-$	$[Er\{N(SiMe_3)_2\}_3Br]^-$	$[Er\{N(SiMe_3)_2\}_3I]^-$
$Er^{(III)}(4f)$	0.74	0.75	0.74	0.70
$Er^{(III)}(5d)$	**0.76**	**0.93**	**0.99**	**1.08**
$Er^{(III)}(6s)$	0.21	0.25	0.26	0.28
$Er^{(III)}(6p)$	**0.61**	**0.73**	**0.77**	**0.84**
X^- (ns)	-0.33	-0.47	-0.48	-0.48
X^- (np)	**-0.57**	**-0.81**	**-0.85**	**-0.93**

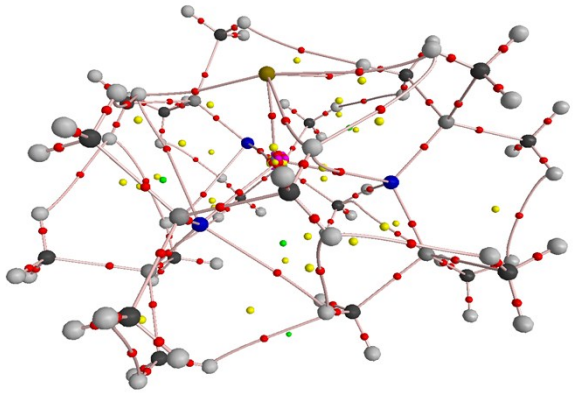

$[Er\{N(SiMe_3)_2\}_3F]^-$

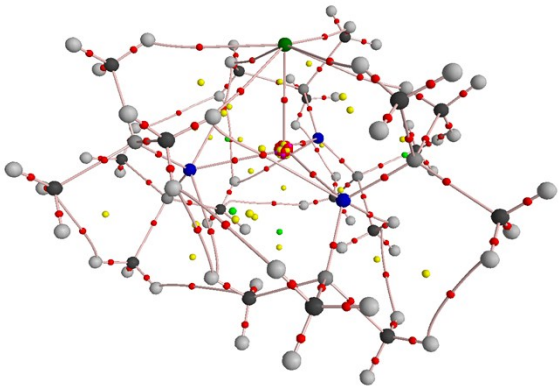

$[Er\{N(SiMe_3)_2\}_3Cl]^-$

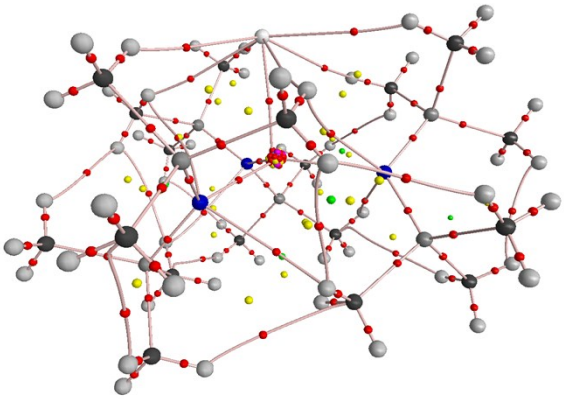

$[Er\{N(SiMe_3)_2\}_3Br]^-$

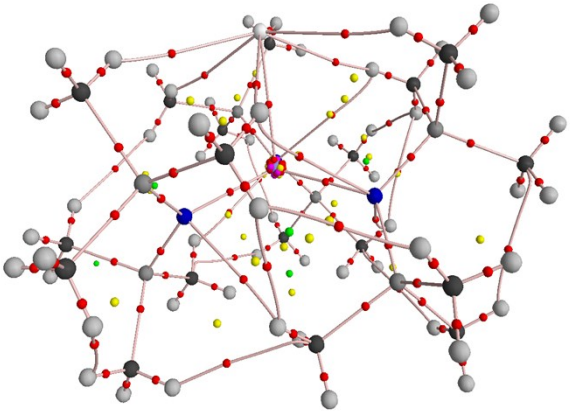

$[Er\{N(SiMe_3)_2\}_3I]^-$

Figure S3. Experimental and ab initio computed molar magnetic susceptibility plots for complex **1**. The black hollow circle represents the experimental magnetic susceptibility extracted from the

experimental data. The coloured lines represent computed magnetic susceptibility at BS1 level of theory.

Energy Decomposition Analysis (EDA)

Table S21. Energy decomposition analysis (in kcal mol^{-1}) of complex **1a** at the B3LYP/TZ2P level. The values in the parentheses give the percentage contribution to the total attractive interactions ($\Delta E_{elstat} + \Delta E_{orb}$)

Fragment Pair	Complex 1a	Pauli repulsion ΔE_{pauli}	Electrostatic interaction ΔE_{elstat}	Total steric interaction	Orbital interactions ΔE_{orb}	Total interaction ΔE_{int}	Total bonding energy
Fragment Pair A	$[Er\{N(SiMe_3)_2\}_3\cdots Cl]^-$	1179.11	-214.51 (20.34)	964.59	-840.04 (79.65)	124.56	124.54
Fragment Pair B	$\{Cl\}\cdots\{Er\cdots\{(NSiMe)3\}$	397.58	-1250.70 (66.50)	-853.12	-630.07 (33.50)	-1483.19	-1483.19

Table S22. Structure of model complex $\mathbf{1_{TP}}$ generated from SHAPE code.

Er	8.845700000	4.215200000	12.419500000
C	5.866944889	0.795726621	9.939975795
H	5.569607889	1.278330621	9.166005795
H	5.183693889	0.182646621	10.216070795
H	6.666496889	0.308406621	9.724983795
Si	7.653131715	3.872741035	9.377930198
C	6.793668889	0.951354621	12.748447795
H	6.080887889	0.364998621	13.015489795
H	7.039202889	1.510986621	13.488471795
H	7.551048889	0.429450621	12.476878795
Cl	7.217900000	4.289600000	14.095500000
C	4.582521889	2.765442621	11.793431795
H	4.264204889	3.303066621	11.064722795
H	4.689928889	3.312498621	12.574190795
H	3.948905889	2.067474621	11.976739795
Si	10.461818185	2.998557240	15.429178156
C	6.009723715	4.488965035	8.700367198
H	6.159171715	4.963709035	7.878872198
H	5.600848715	5.078465035	9.338553198
H	5.430011715	3.742265035	8.537426198
Si	6.227484889	2.006638621	11.332669795
C	8.290708715	2.608853035	8.145914198
H	8.404631715	3.025433035	7.288210198
H	7.658571715	1.888877035	8.068970198
H	9.133621715	2.263013035	8.446903198
Si	7.782688942	7.631468344	12.598593410
C	8.877448715	5.274965035	9.238978198
H	8.964546715	5.535917035	8.320171198
H	9.731657715	4.988861035	9.571649198
H	8.567274715	6.023237035	9.757221198
Si	10.980073027	1.728771179	12.724484917
Si	10.725344379	6.893955189	12.189232330
N	7.284500000	3.293400000	10.944000000
N	10.158100000	2.816900000	13.756200000
N	9.094600000	6.535400000	12.558300000
C	7.476981942	8.073200344	14.384157410
H	6.669544942	8.587244344	14.454312410
H	8.214183942	8.590388344	14.716828410
H	7.390499942	7.269908344	14.902400410
C	10.698567027	0.001143179	13.389148917
H	9.756584027	-0.146624821	13.504565917
H	11.142664027	-0.091604821	14.235537917
H	11.051215027	-0.641804821	12.769066917
C	11.870889379	5.424135189	12.121566330
H	11.610424379	4.848783189	11.399646330

H	11.820590379	4.939959189	12.949850330
H	12.771673379	5.725959189	11.981256330
C	11.333631379	7.981779189	13.594825330
H	12.222424379	8.288319189	13.400201330
H	11.341419379	7.477167189	14.409531330
H	10.749788379	8.737911189	13.689874330
C	11.020943379	7.871739189	10.609834330
H	11.963356379	7.903179189	10.424262330
H	10.687019379	8.766207189	10.718462330
H	10.565762379	7.447299189	9.878862330
C	10.444214027	1.720911179	10.931452917
H	10.522582027	2.605947179	10.569361917
H	9.530438027	1.431663179	10.872612917
H	11.001933027	1.120407179	10.433577917
C	12.829972027	1.923699179	12.642334917
H	13.173847027	1.415943179	11.904573917
H	13.222406027	1.606155179	13.459303917
H	13.048332027	2.851179179	12.524655917
C	8.077520942	9.283640344	11.720522410
H	8.481450942	9.123296344	10.865081410
H	8.660807942	9.829124344	12.252344410
H	7.239231942	9.734804344	11.598316410
C	6.204957942	6.975944344	11.874411410
H	6.320613942	6.826604344	10.932973410
H	5.499404942	7.612604344	12.012458410
H	5.975530942	6.147500344	12.304394410
C	12.158379185	2.450243240	16.058538156
H	12.380730185	1.596647240	15.678342156
H	12.136987185	2.377931240	17.015817156
H	12.819025185	3.096335240	15.802811156
C	10.315425185	4.748507240	15.999698156
H	11.060675185	5.256263240	15.669290156
H	10.310449185	4.773659240	16.959240156
H	9.497350185	5.125787240	15.667027156
C	9.209799185	1.972355240	16.361790156
H	8.326827185	2.308763240	16.185270156
H	9.390103185	2.024231240	17.303227156
H	9.268019185	1.059023240	16.072116156

Table S23. Structure of model complex $\mathbf{1_{TD}}$ generated from SHAPE code.

Er	8.520200000	4.230100000	12.754700000
C	6.041298892	0.999597997	9.876194671
H	5.743961892	1.482201997	9.102224671
H	5.358047892	0.386517997	10.152289671
H	6.840850892	0.512277997	9.661202671
Si	7.682015382	3.926362636	9.232058331
C	6.968022892	1.155225997	12.684666671
H	6.255241892	0.568869997	12.951708671
H	7.213556892	1.714857997	13.424690671
H	7.725402892	0.633321997	12.413097671
Cl	6.922400000	4.306600000	14.405100000
C	4.756875892	2.969313997	11.729650671
H	4.438558892	3.506937997	11.000941671
H	4.864282892	3.516369997	12.510409671
H	4.123259892	2.271345997	11.912958671
Si	10.417088306	2.972791644	15.145536289
C	6.038607382	4.542586636	8.554495331
H	6.188055382	5.017330636	7.733000331
H	5.629732382	5.132086636	9.192681331
H	5.458895382	3.795886636	8.391554331
Si	6.401838892	2.210509997	11.268888671
C	8.319592382	2.662474636	8.000042331
H	8.433515382	3.079054636	7.142338331
H	7.687455382	1.942498636	7.923098331
H	9.162505382	2.316634636	8.301031331
Si	7.997394698	7.451110320	12.581368422
C	8.906332382	5.328586636	9.093106331
H	8.993430382	5.589538636	8.174299331
H	9.760541382	5.042482636	9.425777331
H	8.596158382	6.076858636	9.611349331
Si	11.056169328	1.625344722	12.630911783
Si	10.883986214	6.939963113	12.162555561
N	7.602400000	3.350200000	10.840100000
N	10.269900000	2.908400000	13.443100000
N	9.285900000	6.355200000	12.330700000
C	7.691687698	7.892842320	14.366932422
H	6.884250698	8.406886320	14.437087422
H	8.428889698	8.410030320	14.699603422
H	7.605205698	7.089550320	14.885175422
C	10.774663328	-0.102283278	13.295575783
H	9.832680328	-0.250051278	13.410992783
H	11.218760328	-0.195031278	14.141964783
H	11.127311328	-0.745231278	12.675493783
C	12.029531214	5.470143113	12.094889561
H	11.769066214	4.894791113	11.372969561

H	11.979232214	4.985967113	12.923173561
H	12.930315214	5.771967113	11.954579561
C	11.492273214	8.027787113	13.568148561
H	12.381066214	8.334327113	13.373524561
H	11.500061214	7.523175113	14.382854561
H	10.908430214	8.783919113	13.663197561
C	11.179585214	7.917747113	10.583157561
H	12.121998214	7.949187113	10.397585561
H	10.845661214	8.812215113	10.691785561
H	10.724404214	7.493307113	9.852185561
C	10.520310328	1.617484722	10.837879783
H	10.598678328	2.502520722	10.475788783
H	9.606534328	1.328236722	10.779039783
H	11.078029328	1.016980722	10.340004783
C	12.906068328	1.820272722	12.548761783
H	13.249943328	1.312516722	11.811000783
H	13.298502328	1.502728722	13.365730783
H	13.124428328	2.747752722	12.431082783
C	8.292226698	9.103282320	11.703297422
H	8.696156698	8.942938320	10.847856422
H	8.875513698	9.648766320	12.235119422
H	7.453937698	9.554446320	11.581091422
C	6.419663698	6.795586320	11.857186422
H	6.535319698	6.646246320	10.915748422
H	5.714110698	7.432246320	11.995233422
H	6.190236698	5.967142320	12.287169422
C	12.113649306	2.424477644	15.774896289
H	12.336000306	1.570881644	15.394700289
H	12.092257306	2.352165644	16.732175289
H	12.774295306	3.070569644	15.519169289
C	10.270695306	4.722741644	15.716056289
H	11.015945306	5.230497644	15.385648289
H	10.265719306	4.747893644	16.675598289
H	9.452620306	5.100021644	15.383385289
C	9.165069306	1.946589644	16.078148289
H	8.282097306	2.282997644	15.901628289
H	9.345373306	1.998465644	17.019585289
H	9.223289306	1.033257644	15.788474289

Table S24. Er-X bond lengths in the model $[Er\{N(SiMe_3)_2\}_3X]^-$ model complexes.

Er-X bonds	Bond lengths (Å)
Er—F	2.053
Er—Br	2.67
Er—I	2.88

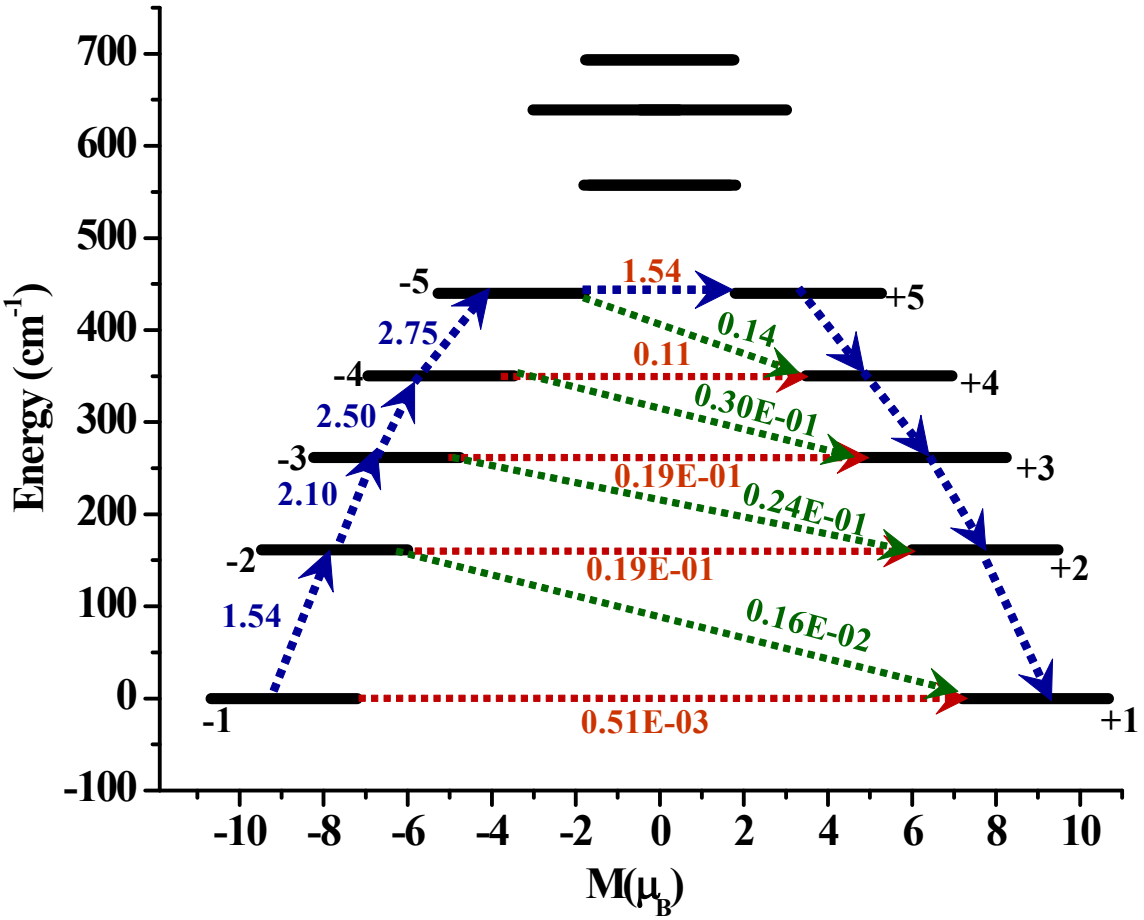

Figure S4. Ab initio blockade barrier for complex **1m**. The thick black line indicates the Kramer's doublets (KDs) as a function of magnetic moment. The green lines show the possible pathway of the Orbach process. The blue lines show the most probable relaxation pathways for magnetization reversal. The dotted red lines represent the presence of QTM/TA-QTM between the connecting pairs. The numbers provided on each arrow are the mean absolute values for the corresponding matrix elements of the transition magnetic moment.

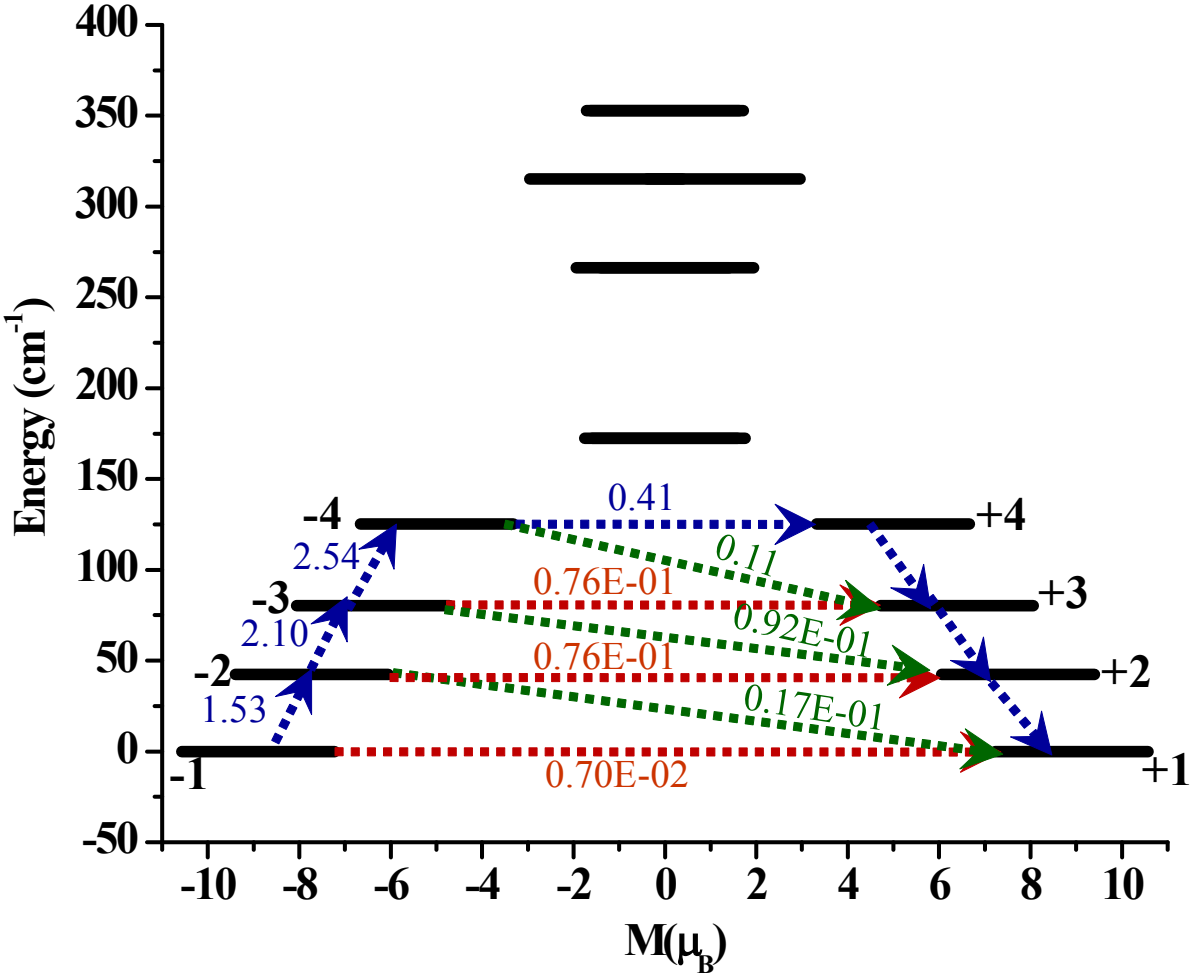

Figure S5. Ab initio blockade barrier for complex **3**. The thick black line indicates the Kramer's doublets (KDs) as a function of magnetic moment. The green lines show the possible pathway of the Orbach process. The blue lines show the most probable relaxation pathways for magnetization reversal. The dotted red lines represent the presence of QTM/TA-QTM between the connecting pairs. The numbers provided on each arrow are the mean absolute values for the corresponding matrix elements of the transition magnetic moment.

τ-out of plane shift parameter

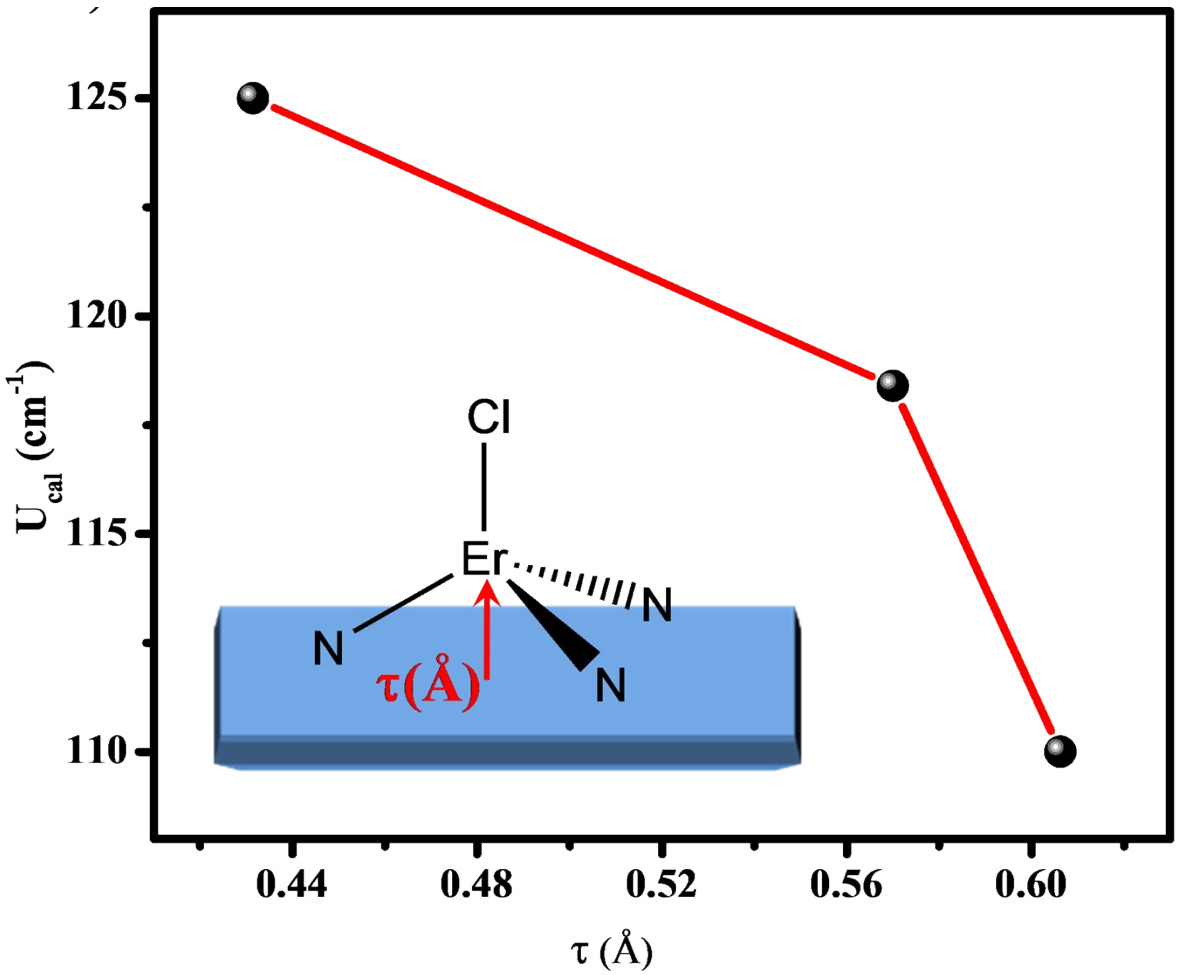

Figure S6. CASSF+RASSI computed U_{cal} value plotted against τ parameter extracted from the experimental geometry of the complexes of **1-3**.

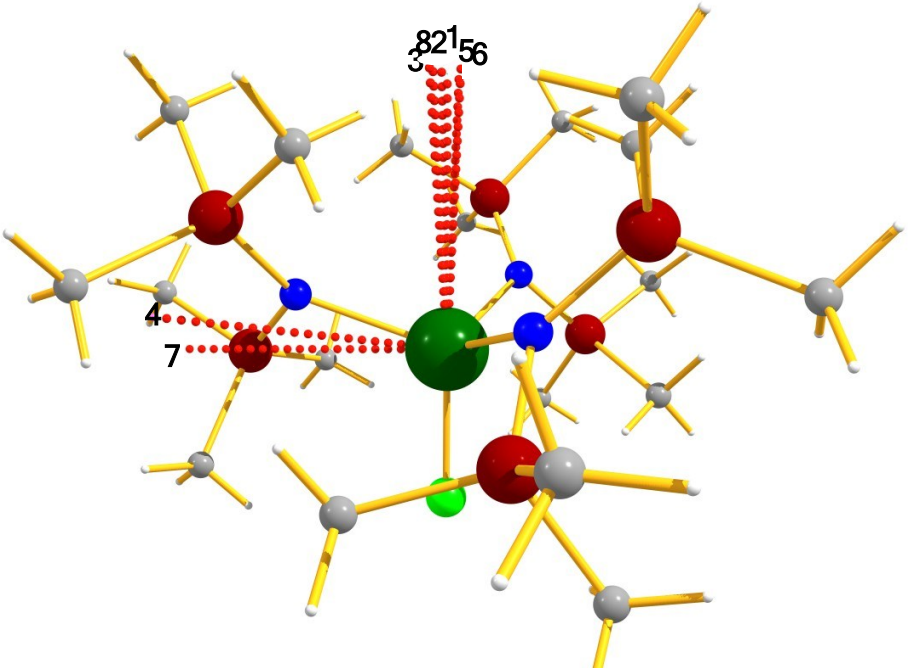

Figure S7. SINGLE_ANISO computed principal magnetization orientation of each KDs of complex $\mathbf{1_{TD}}$.

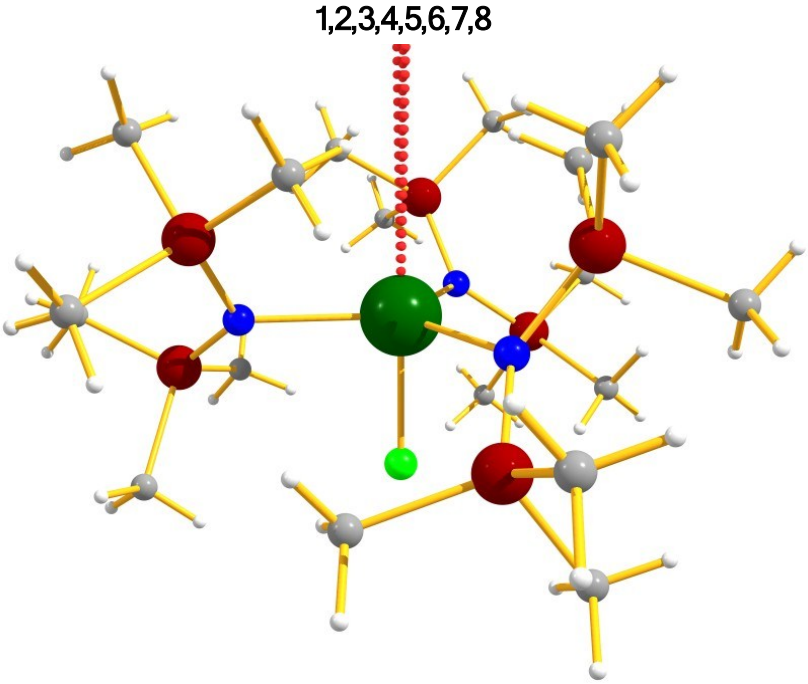

Figure S8. SINGLE_ANISO computed principal magnetization orientation of each KDs of complex $\mathbf{1_{TD}}$.

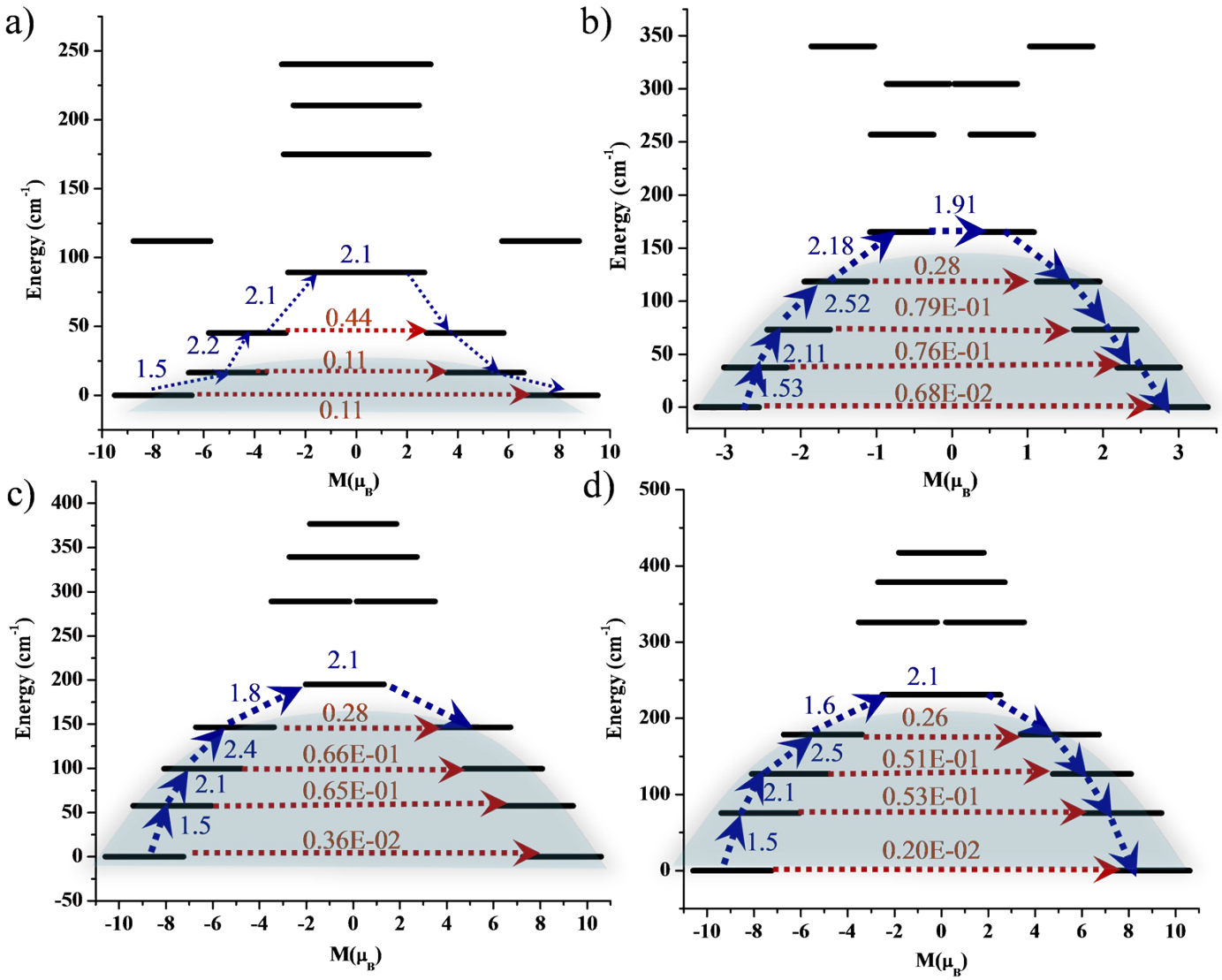

Figure S9. *Ab initio* blockade barrier for complexes $[Er\{N(SiMe_3)_2\}_3X]^-$ a) X=F, b) X=Cl, c) X=Br, d) X=I. The thick black line indicates the Kramer's doublets (KDs) as a function of magnetic moment. The green lines show the possible pathway of the Orbach process. The blue lines show the most probable relaxation pathways for magnetization reversal. The dotted red lines represent the presence of QTM/TA-QTM between the connecting pairs. The numbers provided on each arrow are the mean absolute values for the corresponding matrix elements of the transition magnetic moment.

1. L. Ungur, M. Thewissen, J. P. Costes, W. Wernsdorfer and L. F. Chibotaru, *Inorg. Chem.*, 2013, **52**, 6328-6337.
2. M. J. Frisch, G. W. Trucks, H. B. Schlegel, G. E. Scuseria, M. A. Robb, J. R. Cheeseman, G. Scalmani, V. Barone, B. Mennucci, G. A. Petersson, H. Nakatsuji, M. Caricato, X. Li, H. P. Hratchian, A. F. Izmaylov, J. Bloino, G. Zheng, J. L. Sonnenberg, M. Hada, M. Ehara, K. Toyota, R. Fukuda, J. Hasegawa, M. Ishida, T. Nakajima, Y. Honda, O. Kitao, H. Nakai, T. Vreven, J. A. Montgomery Jr., J. E. Peralta, F. Ogliaro, M. J. Bearpark, J. Heyd, E. N. Brothers, K. N. Kudin, V. N. Staroverov, R. Kobayashi, J. Normand, K. Raghavachari, A. P. Rendell, J. C. Burant, S. S. Iyengar, J. Tomasi, M. Cossi, N. Rega, N. J. Millam, M. Klene, J. E. Knox, J. B. Cross, V. Bakken, C. Adamo, J. Jaramillo, R. Gomperts, R. E. Stratmann, O. Yazyev, A. J. Austin, R. Cammi, C. Pomelli, J. W. Ochterski, R. L. Martin, K. Morokuma, V. G. Zakrzewski, G. A. Voth, P. Salvador, J. J. Dannenberg, S. Dapprich, A. D. Daniels, Ö. Farkas, J. B. Foresman, J. V. Ortiz, J. Cioslowski and D. J. Fox, *Journal*, 2009.
3. A. D. Becke, *J. Chem. Phys.*, 1993, **98**, 5648-5652.
4. T. R. Cundari and W. J. Stevens, *J. Chem. Phys.*, 1993, **98**, 5555-5565.
5. A. Schafer, C. Huber and R. Ahlrichs, *J. Chem. Phys.*, 1994, **100**, 5829-5835.
6. F. Biegler-König and J. Schönbohm, *J. Comput. Chem.*, 2002, **23**, 1489-1494.
7. T. Lu and F. Chen, *J. Comput. Chem.*, 2012, **33**, 580-592.
8. G. te Velde, F. M. Bickelhaupt, E. J. Baerends, C. Fonseca Guerra, S. J. A. van Gisbergen, J. G. Snijders and T. Ziegler, *J. Comput. Chem.*, 2001, **22**, 931-967.
9. K. Morokuma, *J. Chem. Phys.*, 1971, **55**, 1236-1244.
10. T. Ziegler and A. Rauk, *Theor. Chim. Acta.*, 1977, **46**, 1-10.